Control of Surfaces and Heterointerfaces of AlGaN/GaN System for Sensor Devices and Their On-chip Integration on Nanostructures

Hideki Hasegawa

Research Center for Integrated Quantum Electronics (RCIQE) and Graduate School of Information Science and Technology, Hokkaido University, Sappro,060-8628 Japan

E-mail: hasegawa@rciqe.hokudai.ac.jp

Abstract

For successful construction of sensor devices and their future on-chip integration on nanostructures, this paper discusses the present status of understanding and control of surfaces and heterointerfaces of the AlGaN/GaN material system by reviewing a series of works recently carried out by the authors'group.

Leakage currents in Schottky contacts are explained by the authors' thin surface barrier (TSB) model. An important role is played by oxygen shallow donors in leakage in AlGaN Schottky diodes. A large leakage reduction has been achieved by a novel surface control process for oxygen gettering. An unprecedented high sensitivity has been obtained in AlGaN/GaN Schottky diode hydrogen sensor by applying the surface control process. Liquid-phase AlGaN/GaN sensors having an open gate HFET structure show very good pH sensing capability as well as good sensing capability of polar liquids. Finally, the selective MBE growth of AlGaN/GaN nanowire network is discussed as a basic hardware structure for on-chip integration of sensors, paying attention to the heterointerface control.

PACS: 81.05 Ea; 73.40+y;85.30Tv; 81.07Vb;81.15Hi

Keywords: GaN; AlGaN; Sensors: Schottky diodes;HFETs;nanowires;MBE

1. Introduction

In addition to photonic and high-power electronic device applications, the AlGaN/GaN system is attractive as the material for constructing various chemical and bio-chemical sensors due to the following unique features: 1) The bulk and surface properties are chemically stable. 2) A high density two-dimensional electron gas (2DEG) is available near surface which allows highly sensitive detection of surface phenomena. 3) As compared with traditional III-V semiconductors such as GaAs, InP and related ternary and quaternary materials, the material is environment-friendly. 4) Due to large bandgap energies, the material allows sensing operation at high temperatures. 5) Realization of wireless sensor chips seems to be feasible by on-chip co-integration with heterostructure field effect transistor (HFET) circuits for sensor signal processing and wireless communications.

One of the problems of this material system is known to be its relatively high cost as compared with various other sensor materials. However, this demerit may be counterbalanced by the advantage brought by the above feature 5) which will benefit the future ubiquitous network society involving various sensor networks [1].

The AlGaN/GaN material system is also potentially suitable for constructing high temperature operating quantum nanodevices such as single electron transistors (SETs) and quantum wire transistors due to wide energy gaps with a large ΔE_c for strong quantum confinement. In addition, availability of a high density 2DEG even without doping due to intrinsic and piezoelectric polarization is extremely attractive, because it may avoid the doping fluctuation problem in nanodevices. Sensors based on quantum nanostructures will have enhanced sensitivities due to increase of surface-to-volume ratio as well as due to highly charge-sensitive nature of quantum transport. Arrays of nano-scale sensors with high sensitivity and spatially resolved sensing capability in nanospace will be particularly attractive for bio-nano type applications. Nanodevices for sensor signal processing are also attractive

because they should operate at ultralow power levels as compared with the scaled silicon complementary metal oxide semiconductor (CMOS) transistors[2]. Operation with ultra-low power dissipation is one of the essential requirements for constructing intelligent wireless sensor chips by on-chip co-integration.

However, surfaces and heterointerfaces of group III nitrides are still neither well understood, nor well controlled up to now. For example, large leakage currents flow in AlGaN/GaN Schottky diodes and Schottky gates of AlGaN/GaN HFETs. They not only deteriorate performances of power rectifiers and transistors, but also sensor performances, as our initial effort on Schottky diode type hydrogen sensors indicated [3]. AlGaN/GaN HFETs are known to exhibit an instability phenomenon called current collapse which is known to be related to surfaces. As for nanostructure formation for quantum nanodevices, several groups have reported the growth of GaN quantum dots (QDs) using the Stranski-Krastanov (SK) mode [4,5] or the anti-surfactant [6,7]. More recently, growth of arrays of vertically standing GaN-based nanowires have been reported [8,9]. However, it seems to be extremely difficult with these approaches to control the position and size of nanostructures simultaneously and to provide necessary wiring to nanostructures, although these are fundamental requirements for successful on-chip integration of nanodevices. We believe that selective MBE growth method which we successfully developed to formation of GaAs-based [10] and InP-based [11] nanostructures is the most promising approach for high density integration of nano-sensors and nano-transistors.

The purpose of this paper is to discuss the present status of understanding and control of the surfaces and heterointerfaces of the AlGaN/GaN material system from the viewpoint of successful construction of sensor devices and their on-chip integration on nanostructures. For this purpose, a series of works recently carried out by the authors'group are reviewed in addition to general discussion. In Section 2, surface related issues in nitride transistors are

discussed with emphasis on the leakage currents in Schottky diodes. In the Section 3, our recent work nitride-based gas-phase and liquid-phase sensors are presented and their performances are discussed. In Section 4, our recent effort on selective MBE growth of AlGaN/GaN nanowire network for on-chip integration is presented, paying attention to the heterointerface control. A brief summary is given in Section 5.

2. Surface related issues in GaN-based Schottky diodes and AlGaN/GaN HFETs

2.1 Surface-related issues in GaN-based devices

Surface-related issues in GaN-based Schottky diodes and transistors can be summarized as follows. On the free surfaces of GaN and AlGaN, high density surface states exist and they cause charge-discharge transients leading to performance instability such as current collapse and poor long-term reliability. Their charging also reduces the channel conductance, which may become a serious issue particularly in nanostructures and nanodevices. A satisfactory surface passivation technique to cope with these problems has not been established yet, although some encouraging results have been reported for use of Si3N4 [12,13] and Al2O3[14]. At metal-semiconductor interfaces, Schottky barrier heights (SBHs) are much more dependent on the metal work function [15] than other III-V materials, indicating weaker pinning of Fermi level. However, Schottky diodes formed on GaN and AlGaN materials exhibit excess reverse leakage currents that are many orders of magnitude larger than the prediction of the standard thermionic emission (TE) model, although many workers analyze I-V characteristics based on the TE model. Another annoying issues related to metal-semiconductor interface is poor ohmic contacts.

Among above issues, large leakage currents in Schottky diodes and Schottky gates of HFETs are particularly problematic for constructing high performance sensors. In fact, our

initial effort to develop Pt Schottky diode hydrogen sensors on GaN and AlGaN/GaN wafers resulted in only very poor performance at room temperature due to large leakage currents [3].

2.2 Leakage currents in GaN Schottky diodes

As a model which explains large leakage currents in nitride-based Schottky barriers, we have recently proposed a thin surface barrier (TSB) model [16] involving non-intentional donors near the surface as shown in **Fig.1(a)**. Due to presence of ionized high-density donors, the width of the Schottky barrier is greatly reduced, and electrons tunnel though this barrier in the form of a Gaussian beam by the thermionic field emission (TFE) or the field emission (FE) mechanism. Analytic expressions for I-V curves have been derived for a simple rectangular distribution of non-intentional shallow donors [16]. These expressions could explain general behaviour of leakage currents. However, detailed quantitative agreement between theory and experiment were not satisfactory.

To analyze I-V-T curves quantitatively, a computer program has been developed which calculates current through the Schottky barrier with an arbitrary potential profile by a combined mechanism of TE, TFE and FE transport. For the calculation, the following general equation is used..

$$J = \frac{4\pi q m^*}{h^3} \int_0^\infty T(E_x) \times \int_0^\infty \left[f_s(E_p + E_x) - f_m(E_p + E_x) \right] dE_p dE_x \qquad (1)$$

where $T(E_x)$ is the tunneling probability calculated under WKB approximation for $E_x = (h^2/2m^*)\, k_x^2$, i.e., the energy component normal to the Schottky interface, f_s and f_m are Fermi-Dirac distribution functions in the metal and in the semiconductor, respectively, and $E_p = (h^2/2m^*)(k_y^2 + k_z^2)$, i.e., the energy component parallel to the interface.

In order to compare simulation results with experiments, Schottky diodes with various metals have been fabricated on the MOVPE-grown n-GaN and n-$Al_xGa_{1-x}N$ ($0.1< x <0.3$) layers, and their I-V characteristics have been measured in detail as a function of the measurement temperature, T. The resultant I-V-T curves showed varieties of anomalous behaviour including large leakage currents, appearance of current plateaus, large ideality factors, etc.

Attempts have been made to reproduce various measured I-V-T curves quantitatively on computer using the above mentioned program based on the TSB model. Excellent fittings have been obtained particularly for n-GaN Schottky diodes[17,18]. An example is given in **Fig.1(b)** for a Ni/n-GaN diode. Choices of values of the fitting parameters have been found very critical to achieve good fitting in both forward and reverse I-V characteristics at various temperatures, T, by the same set of parameters. Excellent fitting in **Fig.1(b)** has been only possible by assuming that defect donors has an exponentially decaying density distribution with a peak density of $5 \times 10^{18} cm^{-3}$and a characteristic decay depth of 11 nm and that the defect donor is a deep donor with the energy depth of E_{DD} =0.25 eV.

The origin of this donor has been assigned to the nitrogen vacancy (V_N) or a defect related to it on the basis of an X-ray photoelectron spectroscopy analysis of the GaN surface [17]. It is also in agreement with a recent theoretical deep level calculation [19], although other theoretical calculation indicates that the nitrogen vacancy acts as a shallow donor[20]. The simulation program could also reproduce various GaN Schottky I-V curves reported by other workers in the literature [17,18].

2.3 Leakage currents in AlGaN Schottky diodes

In order to develop sensors that can be co-integrated on chip with AlGaN/GaN HFETs circuits, it is desirable to utilize AlGaN surfaces as the sensing surface. Availability of high density 2DEG at AlGaN/GaN is also beneficial to achieve high sensing performance.

However, the rectifying behaviour of the AlGaN Schottky diode has turned out to be much poorer than that of the GaN Schottky diode. Namely, as shown in **Fig.2(a)**, it shows sharply increasing and less temperature-dependent reverse characteristics in spite of the fact that it has a larger SBH value.

Because of these anomalous features of I-V-T curves, our computer simulation has given much poorer quantitative agreements with experiments for AlGaN Schottky diodes, making it practically impossible to reproduce exerimental forward and reverse I-V-T curves only by assuming presence of V_N deep donors.

Then, we have paid attention to presence of oxygen. Recent series of analyses using techniques such as the secondary ion mass spectroscopy (SIMS) have indicated that there exist high-density oxygen atoms in AlGaN [21, 22]. As for its role, there was a theory [23] which predicted that it might act like a deep donor with large lattice relaxation similar to EL2 in GaAs. However, more recent experimental and theoretical investigations on the role of oxygen impurity in GaN and AlGaN have indicated that it is a shallow donor with an activation energy of about 30meV [22, 24]. Thus, it is highly likely that there exist two types of surface donors in the AlGaN layer, namely, V_N deep donors and oxygen shallow donors. Then, fitting for AlGaN Schottky diodes has been carried out by using two exponentially decaying distributions of these two unintentional surface donors[25]. The energy depth of oxygen donor is assumed to be E_{DD}=0.03eV. The best fitting results by using two types of unintentional donors are shown in **Fig. 2 (a)** where the assumed donor distribution and energy depths of donors are shown in **Fig. 2 (b).** Such excellent fittings have been obtained, indicating that the current transport in AlGaN diodes are affected by shallow oxygen donors in addition to deep V_N donors.

3. Nitride-based Gas-phase and Liquid-phase Sensors

3.1 Sensors based on III-V semiconductors and their structures

Recently, interests for developing various high-performance sensors have been increasing, reflecting trends toward sensor networks and novel and rapidly expanding bio-nano applications. III-V compound semiconductors are excellent material candidates for high performance sensors. The attractive features are 1) superb electron transport properties with high surface sensitivity, 2) wide varieties of materials and material selection, 3) availability of various heterostructures with different band line-ups, 4) availability of advanced nanotechnology for forming nanostructures, and 5) oppotunity of on-chip co-integration with signal processing and communication circuits.

Example of III-V sensors reported in literature include gas sensors using Pt or Pd on GaAs [26], InP [27, 28], GaN [3, 29-31] and AlGaN/GaN [3, 32- 34] materials, and liquid and biochemical sensors using GaAs [35,36], AlGaAs/GaAs [37], GaN [38] and AlGaN/GaN [39-41] materials. The device structures used in these sensors are schematically shown in **Fig.3(a).** They are Schottky diodes, open gate (or gateless) field effect transistors (FETs) and ordinary FETs which are familiar in conventional transport devices. An example of a somewhat different configuration is immobilization of single stranded DNA on As-stabilied GaAs(001)[33,34] for possible application to so called DNA chips.

As actual examples, structures of the hydrogen sensor and liquid-phase sensor formed on the AlGaN/GaN system that have been investigated recently by the author' group are shown in **Fig.3 (b)** and **(c)**, respectively. They are a Pd ring Schottky diode structure [34] and an open gate FET structure [41] and both are formed on a standard AlGaN/GaN HFET wafer so that future co-integration with signal processing HFETs is easily accomplished.

For fabrication of the Schotty diode hydrogen sensor shown in **Fig.3(b)**, circular Pd Schottky diodes with Ti/Al/Ti/Au ohmic ring electrodes are formed on an $Al_{0.25}Ga_{0.75}N$/GaN heterostructure grown on sapphire with a sheet carrier concentration of $0.8\text{-}1.0 \times 10^{13}$ cm^{-2} and

a Hall mobility of 1100 cm^2/Vs at RT. Ohmic electrodes are annealed at 800 ^oC for 1 min. Then, Pd Schottky contacts with a thickness of 75 nm and a diameter of 600 μm are formed by electron-beam deposition after surface treatment in HF solution.

For fabrication of the AlGaN/GaN liquid-phase sensor shown in **Fig.3(c)**, processing starts from isolation patterning using an electron-cyclotron resonance (ECR)-assisted reactive ion beam etching with a CH_4-based gas system consisting of CH_4, H_2, Ar and N_2. The addition of N_2 to the gas system is very effective in achieving a smooth and stoichiometric surface [42]. The drain and source electrodes are formed by deposition of Ti/Al/Ti/Au multilayer and annealing. Then, the device surface was covered with SiO_2 film with a thickness of 100 nm using plasma-enhanced chemical vapor deposition (PECVD) at 300 ^oC. The open-gate area having the gate length of 10 μm and the gate width of 500 μm, is formed through photolithography and wet etching processes in a buffered HF solution. Thus, the open gate region is bare, and not intentionally passivated.

3.2 Surface control of AlGaN/GaN wafers

Judging from the discussion given in the previous section, elimination of oxygen from AlGaN layers is highly desirable prior to sensor fabrication in order to realize high performance sensors on AlGaN surfaces. Thus, we have recently attempted to develop a novel surface control process which uses an ultrathin Al layer as a gettering material for oxygen. The sequence of this surface control process is shown in **Fig. 4**. It consists of the following steps: 1) Treatment of AlGaN surface in RF-excited plasma assisted nitrogen radicals at 300 ^oC for 10min. to remove V_N defetcs. 2) Molecular beam deposition of an ultrathin Al layer of 1.5nm at RT in molecular beam epitaxy (MBE) chamber with a very slow deposition rate of ~0.01nm/sec. 3) Annealing of the sample at 700^oC for 10min in UHV. 4) Removal of thin Al layer in HF solution. 5) Electron-beam deposition of Pt or Pd Schottky electrode in the case of

the hydrogen sensor. Steps 1)-3) were carried out in-situ in an ultrahigh vacuum (UHV) multi-chamber system without breaking the UHV condition.

The XPS Al2p spectra taken after Al deposition and after annealing in surface control process are compared in **Fig.5 (a)**. Three different peaks corresponding to Al_2O_3, AlGaN and metallic Al have been observed. The Al_2O_3 peak that exists even immediately after deposition of Al metal in UHV condition is due to the chemical reaction between deposited Al metal and oxygen atoms existing on the AlGaN surface as natural oxide. After the subsequent annealing in UHV, the metallic Al peak disappears completely, indicating that the deposited thin Al metal layer is oxidized completely during the annealing in UHV. Thus, it is highly likely that the Al metal covering the AlGaN surface carry out gettering action of oxygen atoms diffusing from the AlGaN layer, although most of oxygen atoms actually come from decomposition of native Ga_2O_3 on the surface. C-V analysis of the Schttky diode has been also carried out and the result has shown that large reduction of concentration of shallow donors takes place near the surface of the AlGaN layer by the surface control process.

I-V characteristics are compared in **Fig.5(b)** for Pd/AlGaN GaN Schottky diodes fabricated with and without the surface control process. The Schottky diode fabricated without the surface control process exhibits large reverse leakage currents. On the other hand, a remarkable reduction of reverse leakage current of 5 orders of magnitude has taken place by applying the surface control process. The temperature dependences of both forward and reverse currents have also increased, although they are not shown in **Fig. 5(b)**. Thus, the novel surface control process is very effective in reducing the reverse leakage currents in AlGaN Schottky diodes and in Schottky gate of AlGaN/GaN HFETs.

3.3 Performance of AlGaN/GaN gas-phase sensor

Changes of the I-V characteristics caused by exposure to H_2 are shown in **Fig.6 (a)** for the AlGaN/Schottky diode hydrogen sensor shown in **Fig.3(b)** which went through the

surface control process. It showed a large reverse current increase of about five orders of magnitude upon exposure H_2 pressure of 1.0 Torr at V=-1V. On the other hand, current increase has been only one to two orders of magnitude in the diodes without the surface control process. This large improvement of sensitivity is obviously due to reduction of the reverse leakage currents as we expected. In fact, we believe that this sensitivity seems to be the highest ever reported for AlGaN-based Schottky diode type hydrogen gas sensors.

The on-off responses of the reverse current at room temperature have also been measured. Examples of the observed turn-on transients are shown in **Fig.6(b)**. Change of current seems to be exponential when the current is plotted in a logarithmic scale vs. time.

Detailed analysis of the data such as shown in **Fig.6(b)**. has led to the following sensing mechanism: 1)H_2 molecules dissociate on the Pd surface and form atomic hydrogen, H* due to catalytic action of Pd. 2)H* diffuses through the Pd layer and reaches the Schottky interface. 3)H* is adsorbed at adsorption sites at the Schottky interface through a rate equation, including the adsorption time constant, τ_a, desorption time constant, τ_d, and the sheet density of total adsorption sites, N_{ao}. H*-adsorbed sites form an interface dipole layer with a monolayer level thickness. 4) Due to this dipole, Schottky barrier height (SBH) is reduced, leading to increase of currents.

This gives, for the reverse current density $I(t)$ at time t, a relation of

$$\Delta(\log I_0(t)) / \Delta(\log I_0(\infty)) = 1 - \exp(-t/\tau) \qquad (2)$$

where $\tau^{-1} = \tau_a^{-1} + \tau_d^{-1}$, $\Delta(\log I_0(\infty)) = \kappa N_{a0}/(1+\tau_a/\tau_d)$, κ is a constant and Δ represents increment due to hydrogen.

The above equation reproduces the behavior of the data such as (log I) vs. t shown in **Fig.6(b)** extremely well by assuming suitable values of parameters and by assuming presence

of hydrogen storage effect in the Pd layer. The C-V analysis revealed parallel shifts of Schottky/2DEG C-V curves with amount of shifts up to as large as 1,200 mV on 1 Torr H_2 exposure. Parallel shifts directly confirm the dipole-induced reduction of SBH. Apparent discrepancy between large values of C-V shifts and observed changes of reverse current can be explained quantitatively in terms of small SBH sensitivity of thermionic field emission (TFE) currents in the TSB model and of current reduction by tunneling through the interface dipole layer even above SBH. It has been also found that recovery transients are faster in air. This fact and the observed hydrogen pressure dependence of the recovery time constant can be explained by reaction of H* with oxygen at the Pd surface.

3.4 Performance of AlGaN/GaN liquid phase sensor

Figure 7(a) shows typical drain I-V characteristics of the open-gate AlGaN/GaN liquid sensor placed in deionized (DI) water at 24 ^{o}C under dark condition. The gate bias is applied to the electrolyte/AlGaN interface at the open-gate area via a saturated calomel reference electrode (SCE). The device clearly exhibited current saturation and pinch-off behaviour, and I-V characteristics are similar to those of ordinary Schottky-gate HFETs. The observed dependence of drain current on pH is shown in **Fig.7(b)** where measurements are performed in a mixed solution of HCl and NaOH in water with different pH values. The dependence of the open-gate transfer characteristics of the HFET on the value of pH has been measured in the linear region at a small drain bias of 0.2 V. The obtained sensitivity for the surface potential change is 57.5 mV/ΔpH. On the other hand, redox potential change, $\Delta\phi$, due to pH change in an aqueous solution is given by the following Nernstian equation.

$$\Delta\phi = -(2.303\ RT/F)\ \Delta pH \qquad (3)$$

where R is the gas constant and F is Farady constant. This gives a theoretical rate of potential change of 58.9mV/ ΔpH at 24 ^{o}C. Thus, the measured rate of the threshold voltage shift of the AlGaN/GaN sensor HFET vs. pH is very close to the theoretical value of the redox potential shift in the solution. However, the exact mechanism how the redox potential shift is transferred to the change of the threshold voltage of the HFET is not clear yet.

Operation stability and response speeds have been also investigated. The device has shown an acceptable stability with response times of 100 - 200 ms.

It has also been found that the present open-gate device is sensitive to immersion into polar liquids such as methanol and aceton. The observed threshold voltage shift, ΔV, can be roughly explained in terms of the well-known Helmholtz equation.

$$\Delta V = \frac{N_S p(\cos\theta)}{\varepsilon\varepsilon_0} \qquad (3),$$

Here, p is the dipole moment, N_S is the dipole density per unit area, θ is the angle between the dipole and the surface normal, ε is the relative permittivity of the liquid, and ε_0 is the permittivity of free space. The response time has been estimated to be several hundred ms. This response time is much faster than several tens of minutes obtained in similar devices formed on GaAs [35] and GaAs/AlGaAs [38] where surface passivation has been found inevitable to achieve stable operation in contrast to use of the bare surface in the present device. Thus, the results obtained indicate that the present open-gate AlGaN/GaN HEMT is very promising for liquid chemical and bio-chemical sensor applications for recognition of various molecules.

4. Heterointerface control in GaN Nanostructure Growth for On-Chip Integration

4.1 Hexagonal nanowire networks for on-chip integration of sensors

For realization of integrated wireless sensor chips, on-chip integration of nanometer-sized sensors with ultra-low-power electronics and low power wireless communication circuits such as used for radio frequency identification (RFID) chips is required. For the electronics, circuits with much smaller power consumption than Si CMOS circuits are required. For this, we have recently proposed and demonstrated basic feasibility of hexagonal binary decision diagram (BDD) quantum circuit approach [44,45] where a hexagonal nanowire network is controlled by nanometer-scale Schottky gates to perform A-D conversion and BDD logic in the quantum transport mode.

Some examples of the sensing structures which seem to fit in the basic hexagonal BDD hardware architecture are shown in **Fig.8(a)** and **(b)**. **Figure 8(a)** shows a nanometer-scale hexagonal hydrogen sensing head which we plan to fabricate in future on AlGaN/GaN nanowire networks. Here, a bridge is formed by Pd and Al Schottky gate nanowire transistors. In this bridge, hydrogen induces threshold voltage shifts only on Pd-gated devices. Such a structure has been actually fabricated, not yet on AlGaN/GaN, but on InP[46], and it has been confirmed that hydrogen exposure caused no threshold voltage shifts on Al-gated InP FETs in the bridge, indicating proper function of the head.

A possible array structure of sensor FETs having hexagonal BDD hardware architecture is shown in **Fig.8(b)**. This structure allows sensitive detection of the potential distribution of the sensing object in nanometer space. If such a structure with sufficiently high spatial resolution is successfully developed, it may have large application in the bio-chemical applications.

4.2 Selective MBE growth of GaN nanowire networks and heterointerface control

High density hexagonal AlGaN/GaN nanowire networks are required for the integrated sensor chips having the hexagonal BDD archtecture. Following the success of growing GaAs-based [10] and InP-based [11] nanowires by our selective molecular beam epitaxy

(MBE) growth on patterned substrates[13], we have recently succeeded in growing position- and size- controlled AlGaN/GaN nanowire network structures on (0001) pre-patterned GaN substrates by our selective MBE growth method [47,48].

The growth sequence is schematically shown in **Fig. 9(a)**. First, mesa stripes are fabricated as templates for growth by etching of MOVPE grown GaN layer on (0001) sapphire substrates. Since wet etching is difficult for nitride-based materials, etching is carried out by an electron cyclotron resonance assisted reactive ion beam etching (ECR-RIBE) process, developed for nitrides by our group [43]. Then, the AlGaN lower barrier layer is grown by MBE on the patterned substrate with mesa stripes. Growth is typically done at 800°C and under the irradiation of the N_2 radical excited with a microwave power of 350W and the N_2 flow rate of 0.5sccm. Subsequent growth of GaN results in a self-organized formation of a GaN wire due to built-in growth selectivity. Finally, the top AlGaN barrier layer is formed. Typical SEM images of QWR structures grown on the <11-20>-oriented mesa are shown in **Fig.9(b)**.

To clarify the evolution of the cross-sectional heterointerface structure of the nanowire, GaN/AlGaN nanowires have been grown repeatedly on the same mesa-patterned substrate with growth markers. It has been found that planar boundaries separating the region grown on the top (0001) facet from those grown on the side (1-101) facets appear during growth, and they determine the width of the wire. We called these boundaries as facet boundary planes (FBPs) [10] in our previous study of the selective MBE growth of GaAs-based QWRs. They are schematically shown by dashed lines on the right figure of **Fig.9(a).** FBPs do not correspond to any of high index facets, but their evolution is due to the kinetic process involving the growth selectivity between the top and the side facets. Then, the lateral width of the QWR is given by the following equation.

$$W - W_0 = -\frac{2r_{top}}{\tan\theta_b} t, \qquad (3)$$

where the W_0 is the lateral width of the GaN buffer mesa on which AlGaN barrier layer is grown, t is the growth time, r_{top} is the growth rate on the top facet, and θ_b, is the angle of FBP with respect to the (0001) surface. θ_b is one of the most important parameters for control of the wire size.

Another important parameter for growth of the present QWR is the growth selectivity on the top facet vs. growth on side facets. To quantify this**,** the growth rate ratio between the top and side facets, r_{top}/r_{side}, have been measured for many samples grown by changing the Al composition and the wire orientations. Here, r_{side} is the growth rate in the direction perpendicular to the side facet surface. For all the samples, the growth rate ratio has been found much larger than unity, indicating presence of large growth selectivity. As for the wire orientation, the <11-20>-orientation is suitable to obtain the high growth selectivity as compared with the <1-100>-orientation. This can be also explained by the difference of the incorporation rate and the migration length on the different crystalline facets.

Using the basic data for growth and a hexagonal substrate pattern shown in **Fig.10(a)**, initial attempts to grow hexagonal networks have been made, and an example of grown sample is shown in **Fig.10(b)**. This sample gave strong photoluminescence from the wire region. Although the hexagonal pitch is still very large, there is no reason which prevents further size reduction. Since hexagon densities of 10^8-10^9/cm^2 have been achieved in GaAs- and InP- based material systems, similar densities should be feasible for the AlGaN/GaN system.

5. Summary

From a viewpoint of successful construction of sensor devices and their on-chip integration using nanostructures, this paper has discussed the present status of understanding and control of surfaces and heterointerfaces of the AlGaN/GaN material system by reviewing a series of works recently carried out by the authors'group. Main points of discussion can be summarized as follows.

(1)Large leakage currents in GaN and AlGaN Schottky diodes which deteriorate sensor performances can be explained by the authors' thin surface barrier (TSB) model.

(2) An important role is played by oxygen shallow donors in increasing leakage current in AlGaN Schottky diodes.

(3)A large leakage reduction in AlGaN Schottky diodes can be achieved by a novel surface control process for oxygen gettering.

(4) By applying the surface control process, an unprecedented high sensitivity has been obtained in AlGaN/GaN hydrogen sensor having a Schottky diode structure

(5) Liquid-phase AlGaN/GaN sensors having an open gate HFET structure show very good pH sensing performance as well as good sensing capability of polar liquids.

(6) A hexagonal nanowire networks implementing the BDD architecture is a promising basic structures for on-chip integration of sensors and other functions. Growth of such network on the AlGaN/GaN system is feasible by applying the selective MBE growth method developed by the author's group.

Finally, some basic issues seem to remain still unsolved for further progress in future. They include band line-ups between semiconductors and HOMO/LUMO levels of molecules in liquids and organic materials, origin and properties of surface states in atomic scale, their hybridization with HOMO/LUMO levels of molecules, atomic level structures of various interfacial dipoles that appear in gas-phase and liquid-phase sensors, roles of thin native oxides in sensor performances etc.

Acknowledgment

The author would like to express his sincere thanks to the members of his research group, particularly, Professor T. Hashizume, Professor T. Sato, and Professor M. Akazawa for their research collaboration and fruitful discussions. This work is supported in part by a Grant-in-Aid for Scientific Research (Basic Research (B) #18360002 : Head Investigator H. Hasegawa) from MEXT, Japan.

References

[1] Intel web site, http://www.intel.co.jp/research/ exploratory/wireless_sensors.htm

[2] H. Hasegawa, S. Kasai and T. Sato, International Journal of High Speed Electronics and Systems, 16(2006), 421.

[3] K. Matsuo, T. Hashizume and H. Hasegawa: Appl. Surf. Sci. **244** (2005) 273.

[4] M. Miyamura, K. Tachibana, T. Someya and Y. Arakawa: J. Cryst. Growth, 237-239 (2002) 1316.

[5] J. Brown, F. Wu, P. M. Petroff and J. S. Speck: Appl. Phys. Lett., 84 (2004) 690.

[6] H. Hirayama, S. Tanaka, P. Ramvall and Y. Aoyagi: Appl. Phys. Lett., 72 (1998) 1736.

[7] S. Tanaka, M. Takeuchi and Y. Aoyagi: Jpn. J. Appl. Phys., 39 (2000) L831.

[8] B. Liu,Y. Bando, C. Tang, F. Xu and D. Golberg, Appl. Phys. Lett. 73(1998)3700.

[9] T. Kykendall, P. Pauzuskie, S. K. Lee, Y. Zhang and P. Yang, Nano Lett. 3(2003) 1063.

[10] T. Sato, I. Tamai, S. Yoshida and H. Hasegawa: Appl. Surf. Sci., 234 (2004) 11.

[11] H. Hasegawa, H. Fujikura and H. Okada, MRS Bulletin, 24(1999), pp.25-30.

[12] B.M. Green, K. K. Chu, E.M. Chumbes, J.A. Smart, J.M. Shealy and L.F. Eastman, IEEE Electron Dev. Lett. 21(2000), 268.

[13] T. Mizutani, Y. Ohno, M. Akita, S. Kishimoto, and K. Maezawa, phys. stat. sol. (a) 194(2002), 447.

[14] T. Hashizume, S. Ootomo and H. Hasegawa, Appl. Phys. Lett. 83(2003), 2952.

[15] H. Hasegawa, Y. Koyama and T. Hashizume, Jpn. J. Appl. Phys. 38(1999) 2634.

[16] H. Hasegawa and S. Oyama, J. Vac. Sci. Technol B **20**, 1647-1655(2002).

[17] T. Hashizume, J. Kotani and H. Hasegawa, Appl. Phys. Lett. 84(2004), 4884

[18] J. Kotani, T. Hashizume and H. Hasegawa, J. Vac. Sci. Technol B, 22 (2004) 2179.1. 10.

[19] E. Yamaguchi and M. R. Junnarkar, J. Cryst. Growth 189-190(1998)570.

[20] J. Neugebauer and C. G. Van de Walle, Phys. Rev. B50(1994) 8047.

[21] J. E. Van Nostrand, J. Solomon, A. Saxler, Q.-H. Xie, D. C. Reynolds and D. C. Look, J. Appl. Phys. 87(2000), 8766.

[22] Klaus H. Ploog and Oliver Brandt, J. Vac. Sci. Technol A 16(1997), 1609.

[23] Chris G. Van de Walle, Phys. Rev. B 57(1998), 2033.

[24] H. Wang and A.-B. Chen, J. Appl. Phys. 87(2000), 7859.

[25] J.Kotani, M. Kaneko, H. Hasegawa and T. Hashizume, J.Vac.Sci.Technol.B24(2006)2148.

[26] M. Jaegle and L. Steiner, Sensors and Actuators B 34(1996)543.

[27] H-I. Chen, Y-I Chou and C-Y Chu, Sensors and Actuators B 85(2002)10.

[28] T. Kimura, H. Hasegawa, T. Sato and T. Hashizume, to appear in Jpn. J. Appl. Phys. 44(2006)3414.

[29] B.P Luther, S. D. Wolter and S.E. Mohoney, Sensors and Actuators B 56(1999)164.

[30] J. Schalwig, G. Muller, O. Ambacher and M. Stutzmann, phys.stat.sol.(a) 185(2001)39.

[31] J. Kim, B.P. Gila, G.Y. Chung, C.R.abernathy, S. J. Pearton and F. Ren, Solid-State Electronics 47(2003) 1069.

[32] J. Schalwig, G. Muller, M. Eickhoff, O. Ambacher and M. Stutzmann, Sensors and Actuators B87(2002)425

[33] B.S. Kang, F. Ren, B.P.Gilla. C.R.Abernathy and S.J. Pearton, Appl. Phys. Lett. 84(2004)1123.

[34] K. Matsuo, T. Kimura, H.Hasegawa and T. Hashizume, e-J. Surf. Sci. Nanotech. **3** (2005) 314.

[35] S. Bastide, R. Butruille, D. Cahen, A. Dutta, J. Libman, A. Shanzer, L. Sun, and A. Vilan, J. Phys. Chem. B **101**, 2678(1997).

[36] L. Mohaddes-Ardaballi, L. J. Martinez-Miranda, J. Silverman, A. Christou, L. G. Salamanca-Riba, M. Al-Shenkhly, W.E.Bentley and F. Ohuchi, Appl. Phys. Lett. 83(2003)192.

[37] M. Al-Shenkhly, D. Sweet, L. Salamanca-Riba, B. Varughese, J. Silverman, A. Christou, W.E.Bentley and F. Ohuchi, IEEE Trans. Device and Materials Reliability, 4(2004)192.

[38] S. M. Luber, K. Adlkofer, U. Rant, A. Ulman, A. Golzhauser, M. Grunze, D. Schuh, M. Tanaka, M. Tornow and G. Abstreiter, Physica E 21 (2004) 1111.

[39] S. Steinhoff, M. Hermann, W. J. Schaff, L. F. Eastman, M. Stuzmann and M. Eickhoff, Appl. Phys. Lett. 83(2003)177.

[40] R. Neuberger, G. Muller, O. Ambacher and M. Stutzmann, phys. Stat. sol.(a) 185(2001) 85.

[41] B. S. Kang, F. Ren, L. Wang, C. Lofton, W.W Tan, S. J. Pearton, A. Dabiran, A. Osisnsky and P. P. Chow, Appl. Phys. Lett. 87(2005)023508

[42] T. Kokawa*, T. Sato, H. Hasegawa and T. Hashizume, J. Vac. Sci. Technol. B24 (2006) 1972.

[43] H. Hasegawa, T. Muranaka, S. Kasai and T. Hashizume: Jpn. J. Appl. Phys. 42 (2003) 2375.

[44]H. Hasegawa and S. Kasai, Physica E, vol.11(2001), 149.

[45]S. Kasai, M. Yumoto and H. Hasegawa, Solid State Electronics.,.47(2003),.199

[46]. T. Kimura, H. Hasegawa, T. Sato and T. Hashizume, presented at 2006 IPRM Conf. May 8-12, 2006, Princeton,USA

[47] T. Oikawa, F. Ishikawa, T. Sato, T. Hashizume and H. Hasegawa: Appl. Surf. Sci., 244 (2005)84.

[48] T. Sato, T. Oikawa and H. Hasegawa: Jpn. J. Appl. Phys., 44 (2005) 2487

Figure Captions

F**ig.1** (a)Thin surface barrier (TSB) model and (b)measured and simulated I-V-T curves for Ni/n-GaN Schottky diodes.

Fig.2 (a) Measured and simulated I-V-T curves for Ni/n-AlGaN Schottky diodes, and (b) distributions and energy depths of unintentional donors used in the simulation.

Fig.3 Structures of (a) III-V sensors, (b) AlGaN/GaN hyrogen sensor diode used by the author' group and (c) AlGaN/GaN liquid sensor having an open gate HFET structure used by the author' group.

Fig.4 A novel surface control process for gettering oxygen from AlGaN layers.

Fig.5 (a) In-situ XPS spectra taken on AlGaN surface after Al deposition and after UHV annealing, and (b) effect of the surface control process on I-V characteristics of a Pd/AlGaN Schottky diode.

Fig.6 (a)I-V characteristics and (b) turn-on transients of a hydrogen sensing Pd/AlGaN/GaN Schottky diods subsected to the surface control process.

Fig.7 (a) I-V characteristics and (b) pH-sensing characteristics of a AlGaN/GaN liquid-phase sensor having an open gate strucgture.

Fig.8 (a) Hydrogen sensor head and (b) an array of sensor FETs to detect spatial distributions of potential that are suitable for on-chip integration with circuits under the hexagonal BDD architecture formed on hexagonal nanowire networks

Fig.9 (a) Sequance for selective MBE growth of nanowires and (b) SEM images of grown AlGaN/GaN nanowires.

Fig.10 (a) A substrate pattern for growth of AlGaN/GaN hexagonal nanowire networks and (b) a SEM image of a grown network.

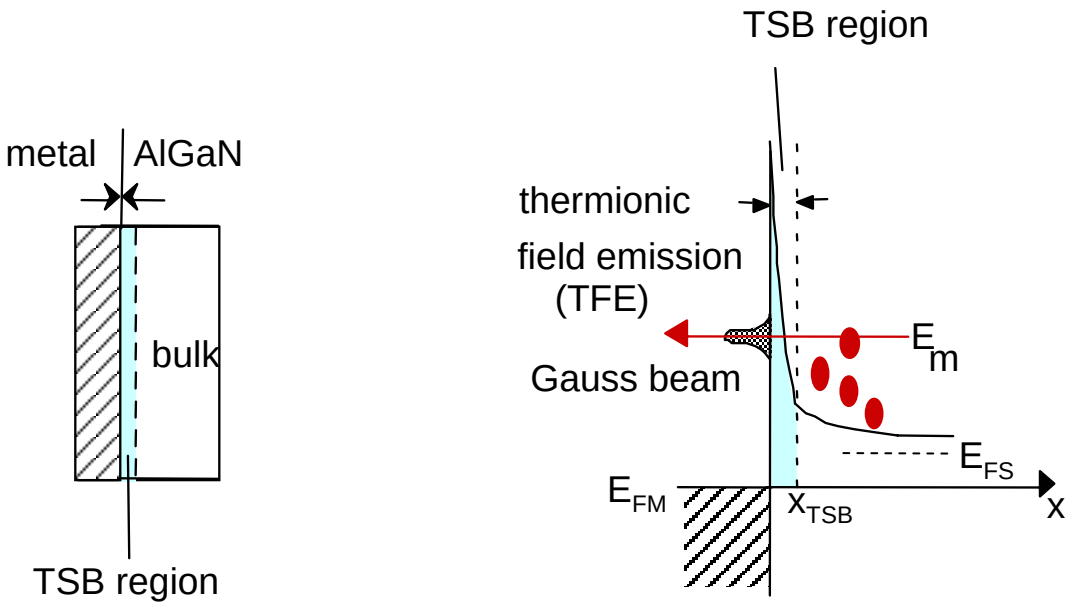

(a)

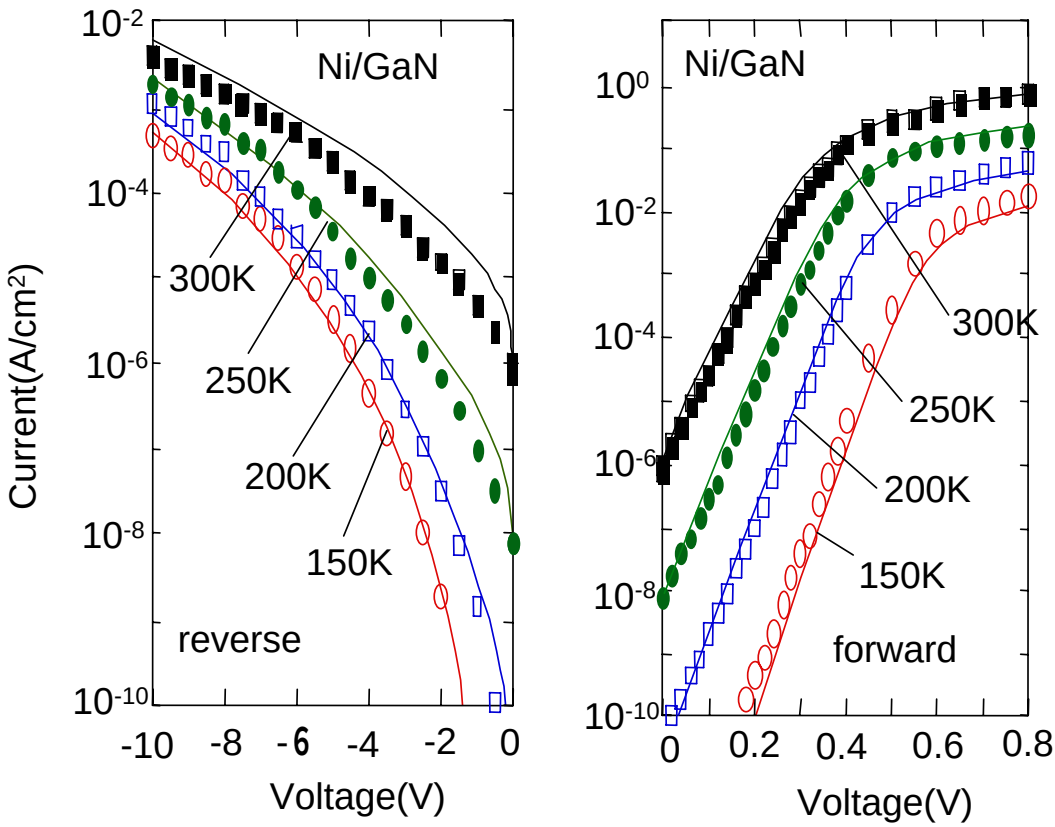

(b)

Fig.1 Hasegawa

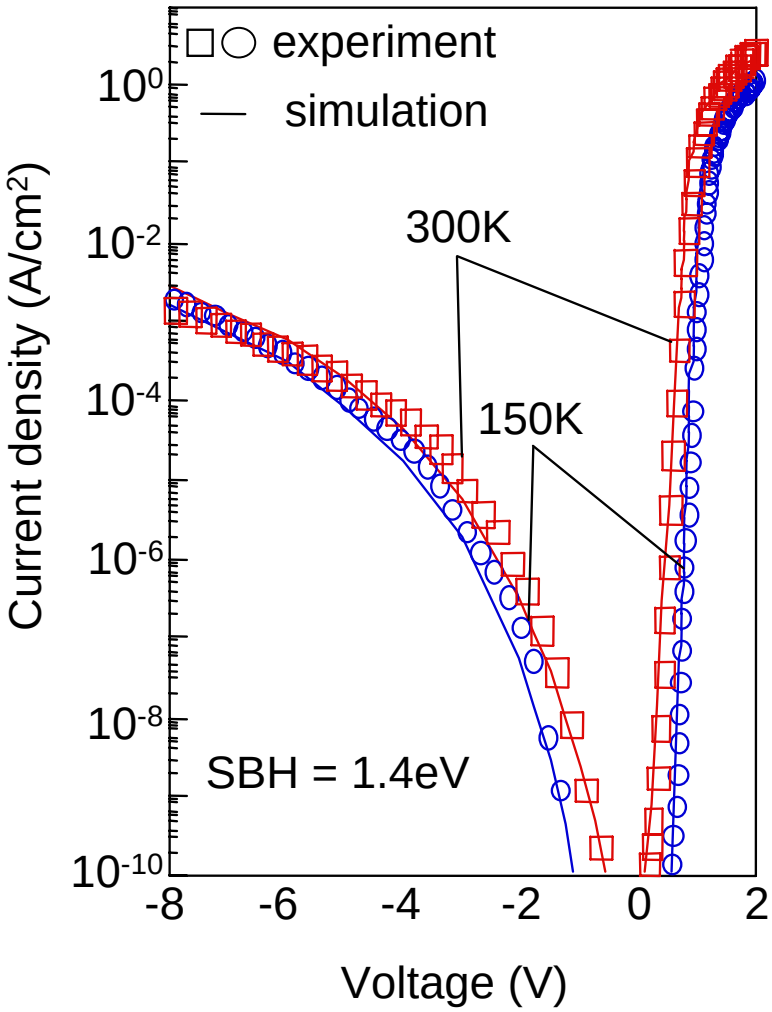

(a)

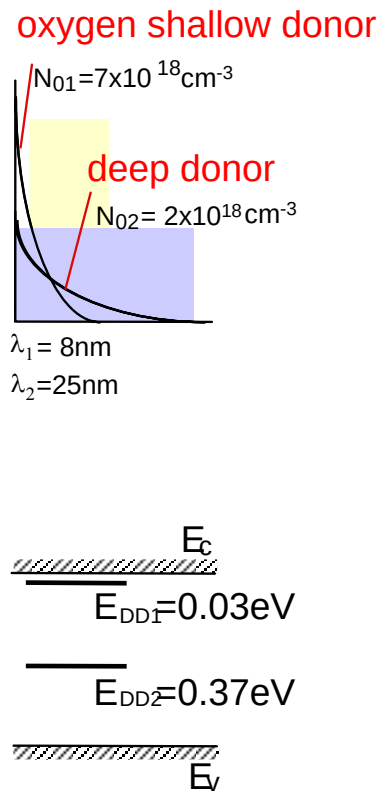

(b)

Fig.2 Hasegawa

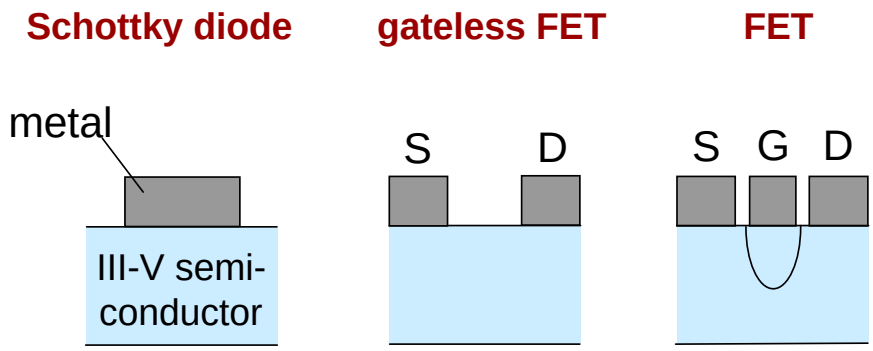

(a)

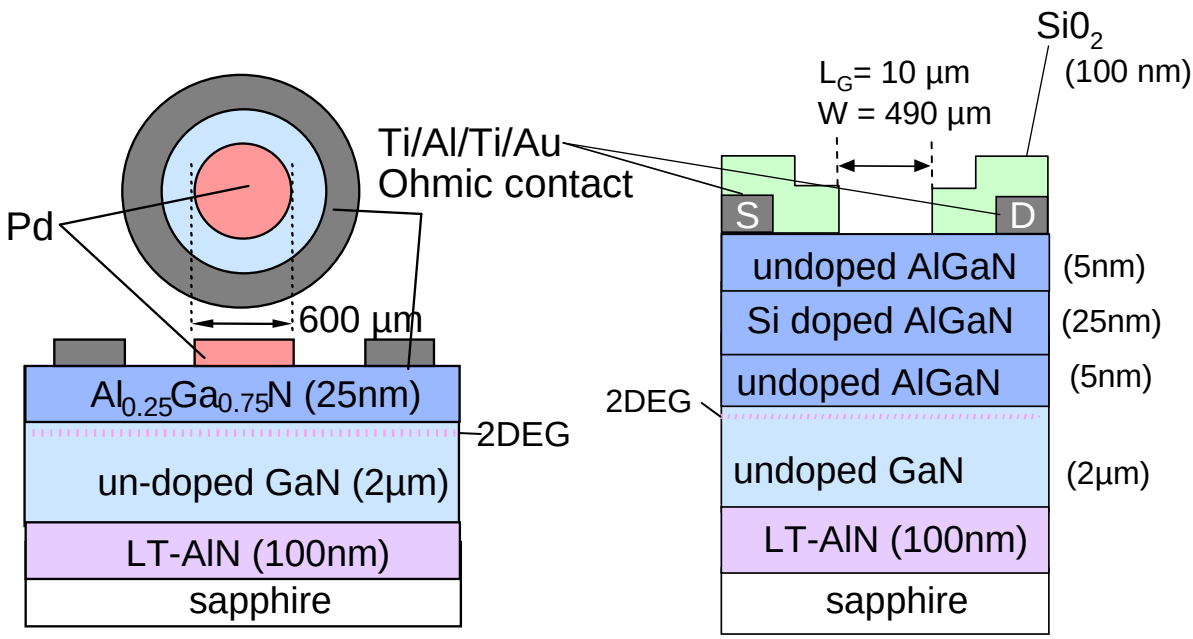

(b)

(c)

Fig.3 Hasegawa

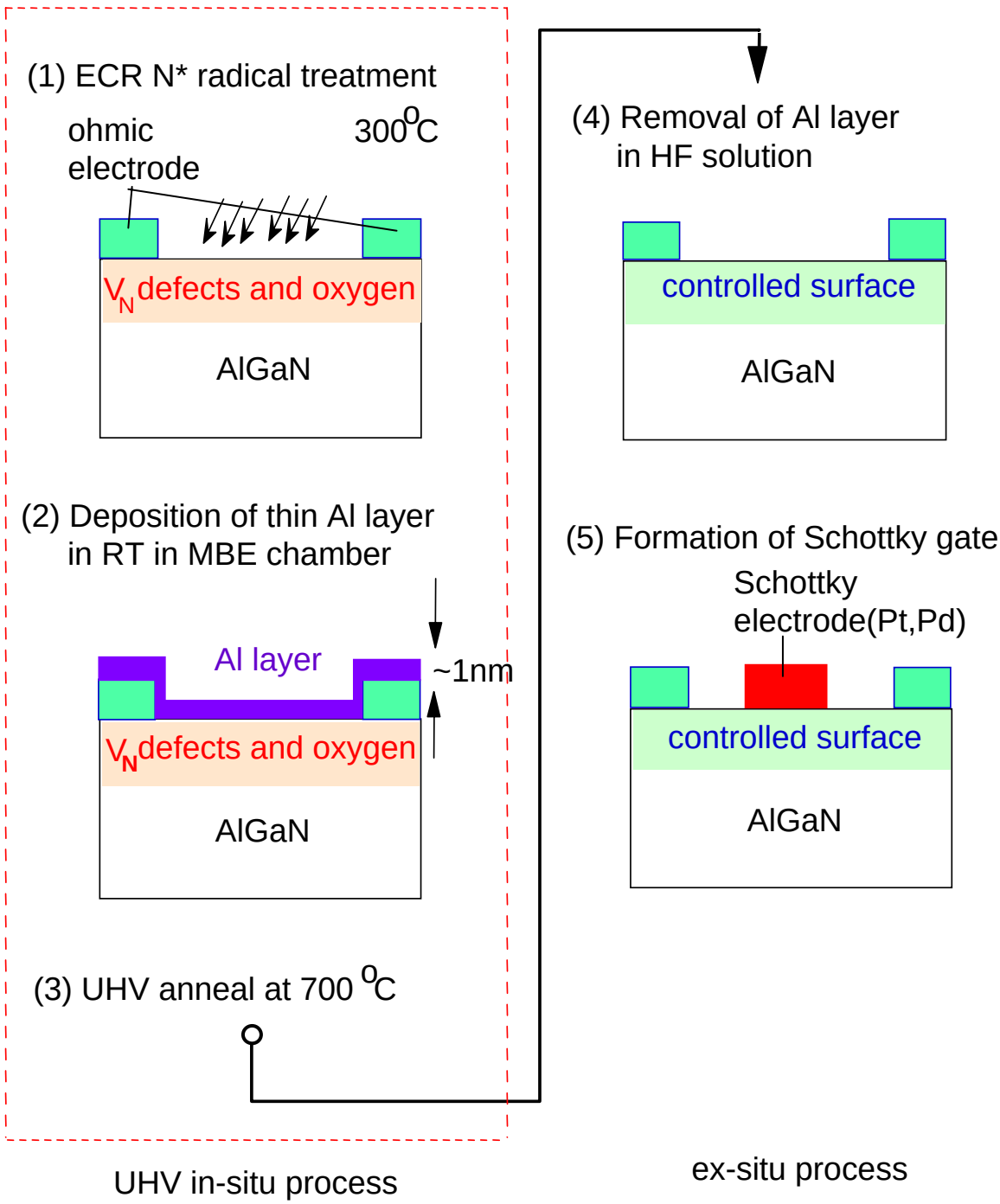

Fig.4 Hasegawa

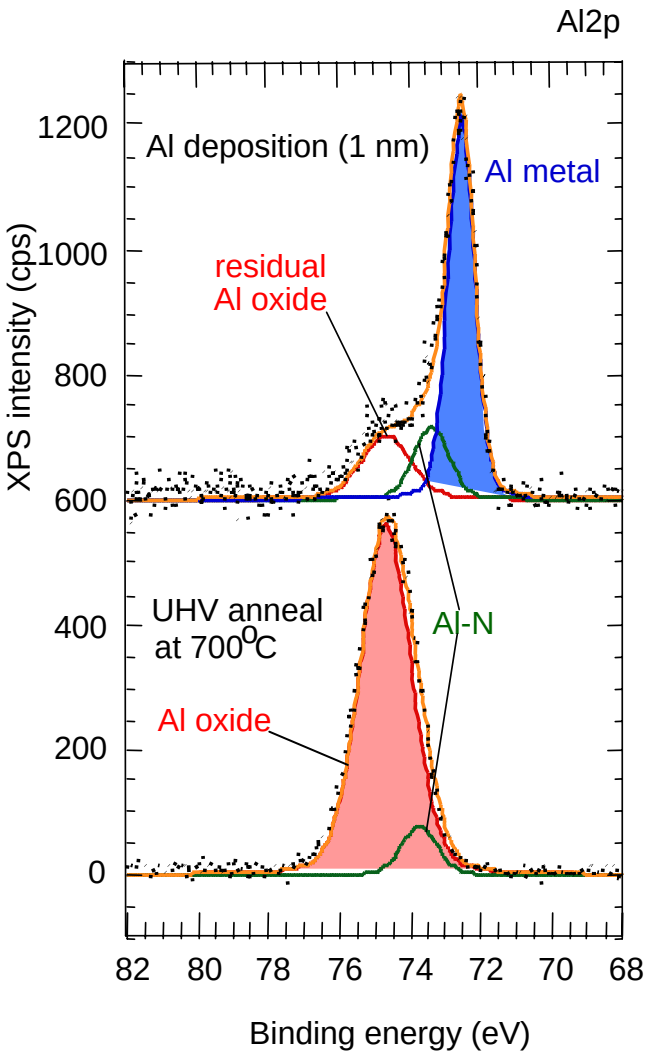

(a)

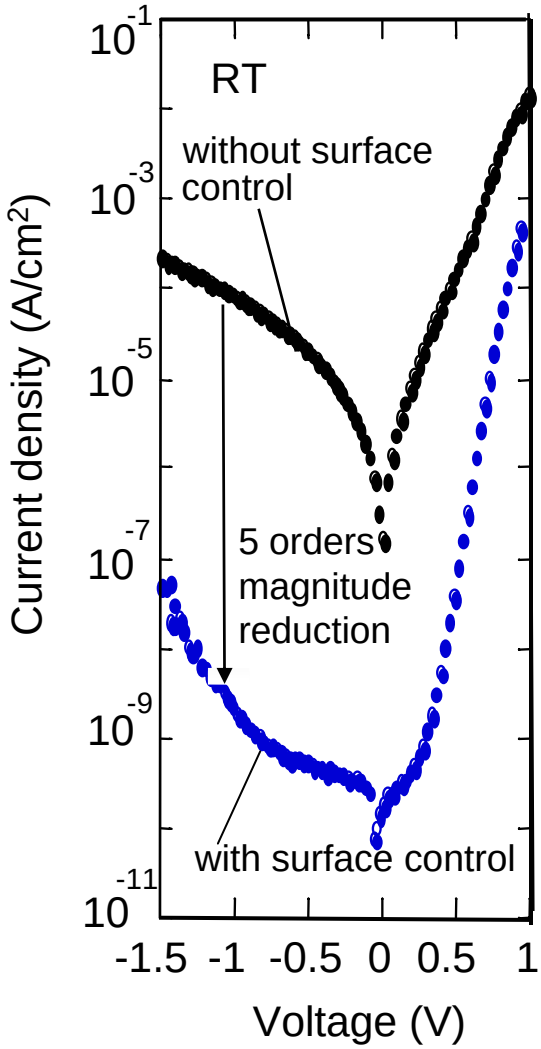

(b)

Fig.5 Hasegawal

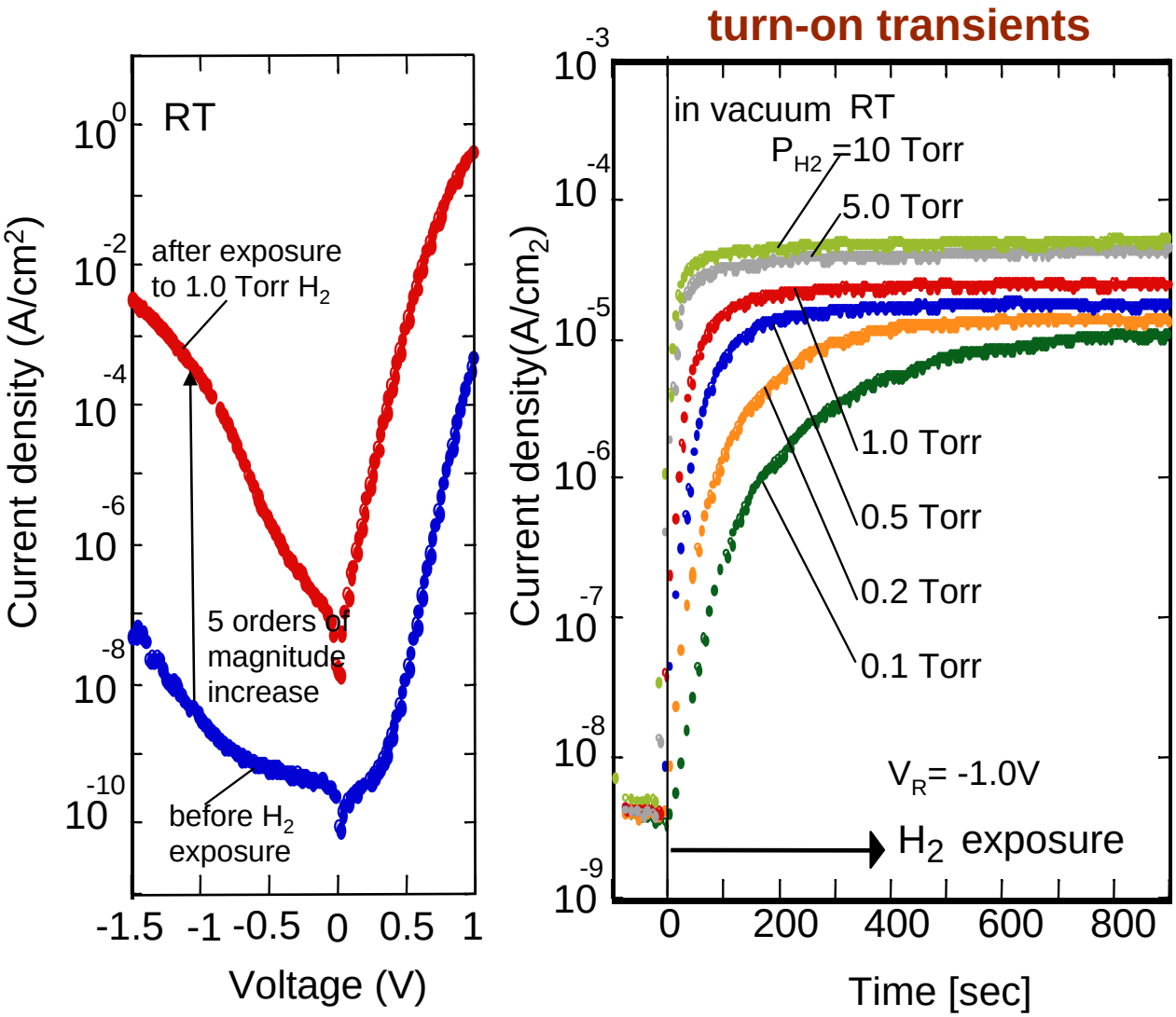

(a) (b)

Fig.6 Hasegawa

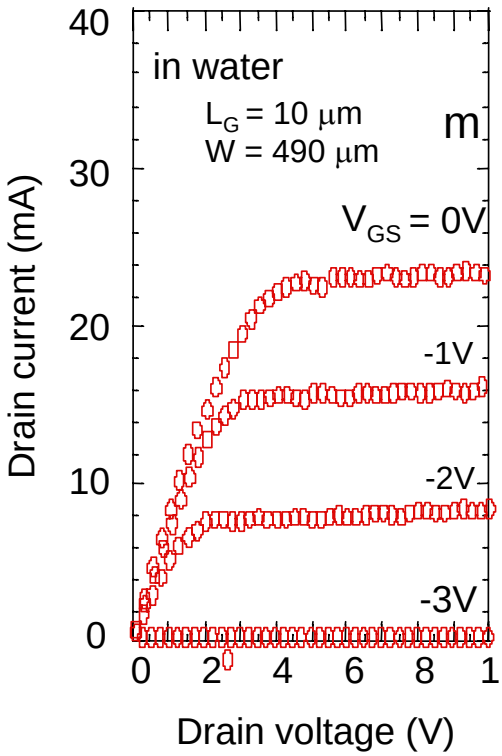

(a)

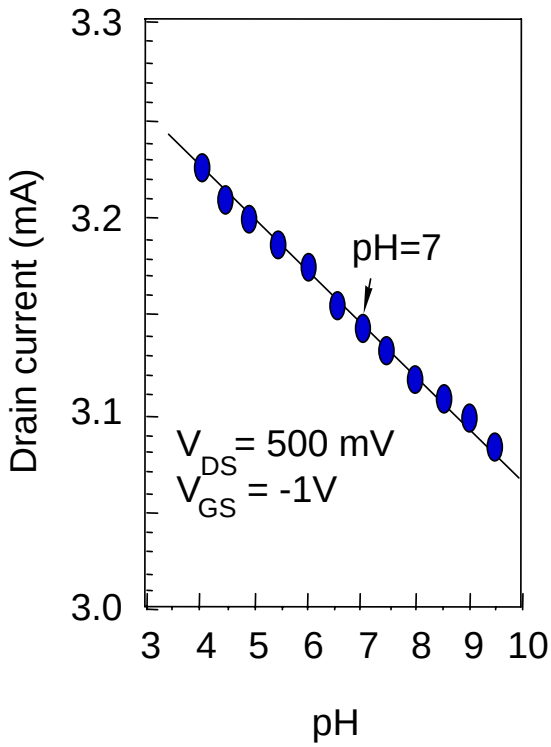

(b)

Fig.7 Hasegawa

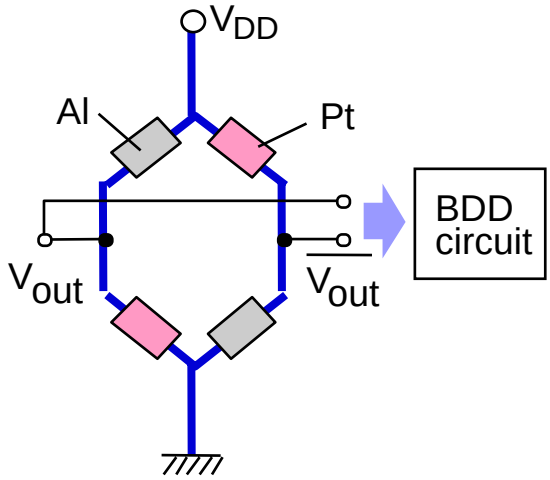

(a)

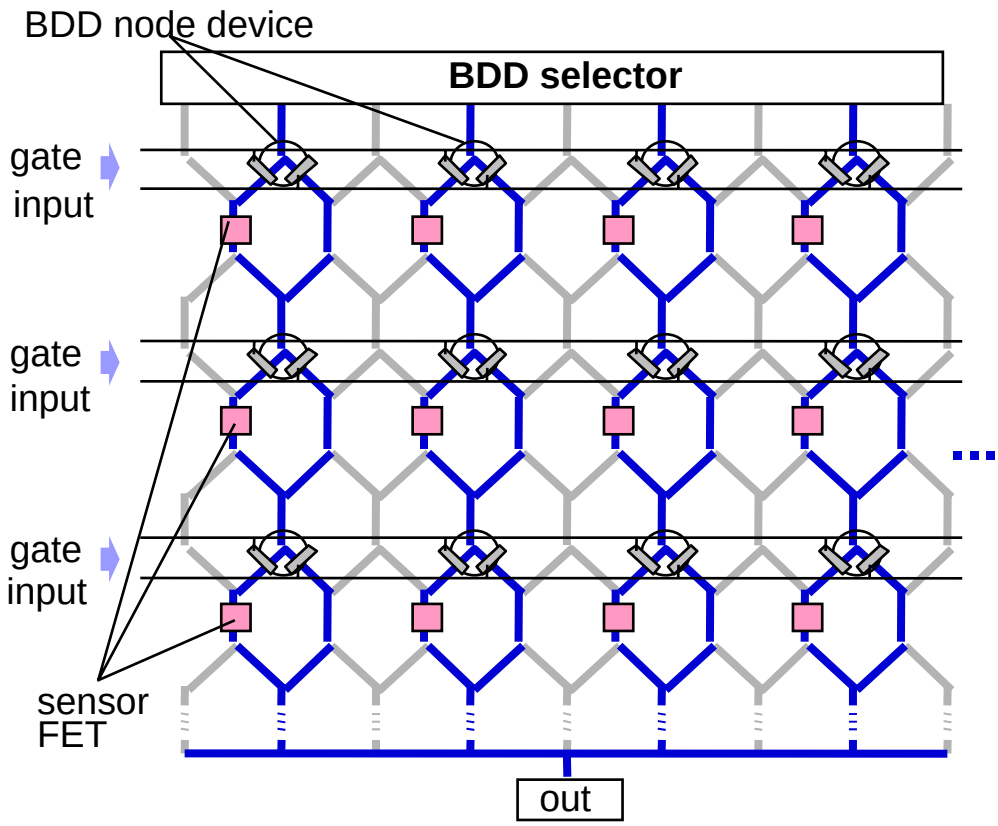

(b)

Fig. 8 Hasegawa

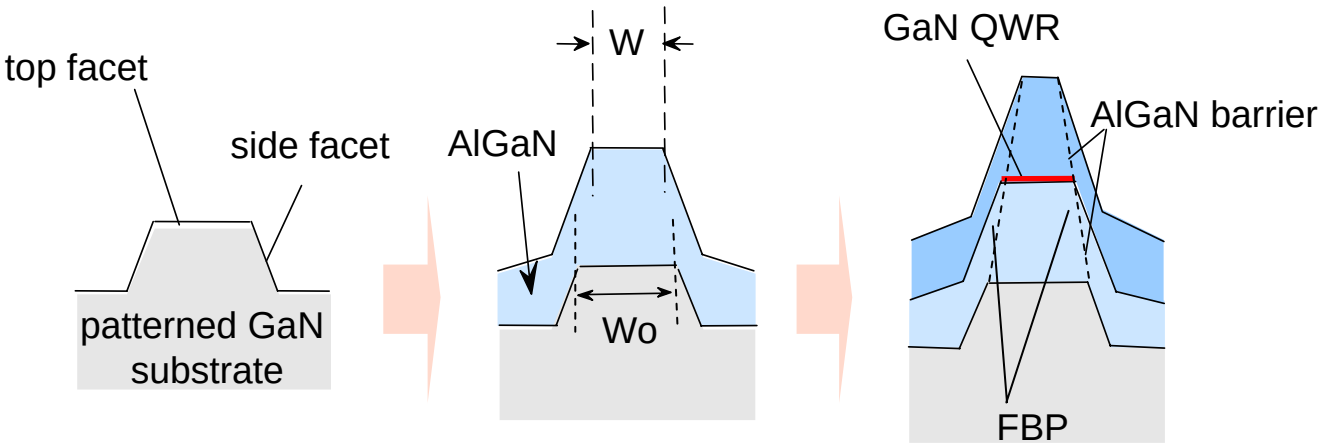

(a)

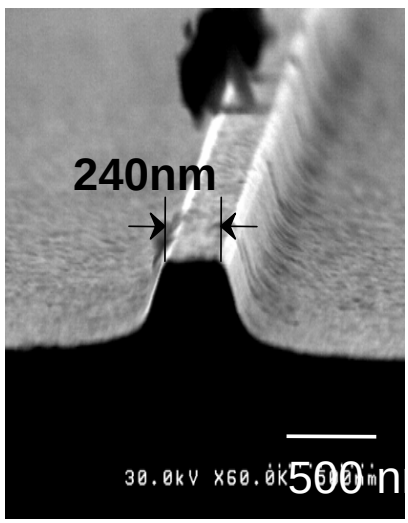

Wo = 350 nm

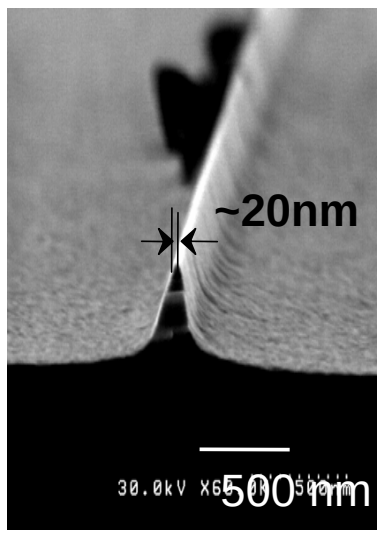

Wo = 50 nm

(b)

Fig.9 Hasegawa

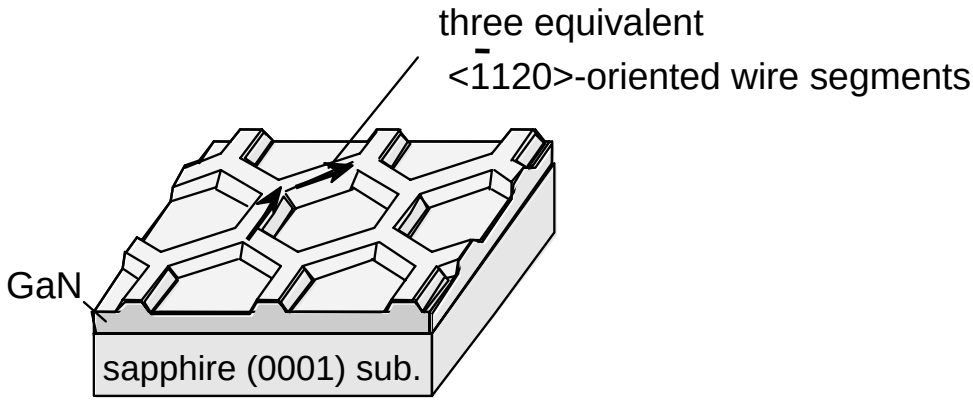

(a)

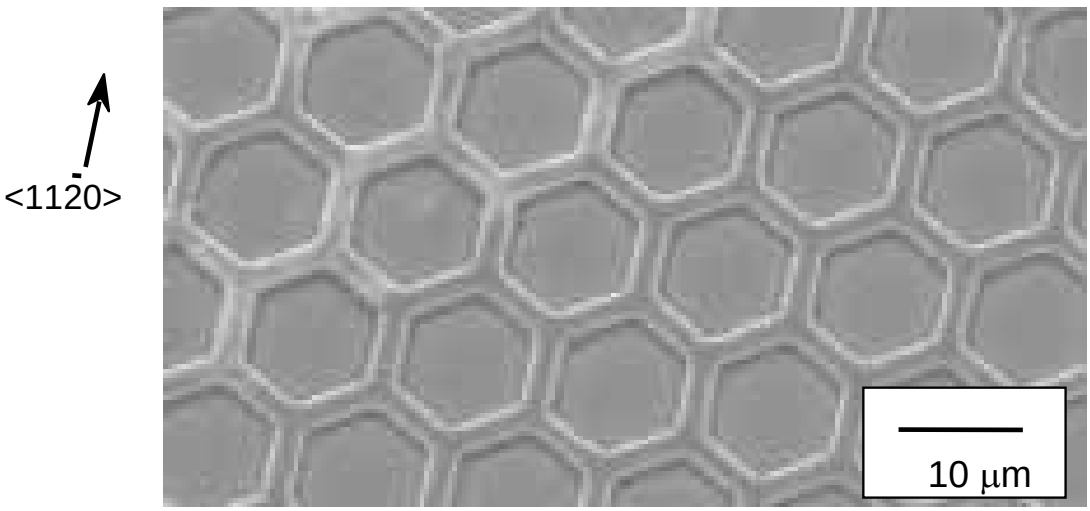

(b)

Fig.10 Hasegawa